# Experimental investigations of the variance and fluctuation spectra of intensity of a laser beam crossing the supersonic gas flow

**V.A. Banakh,[1] V.I. Zapryagaev,[2] I.N. Kavun,[2] V.M. Sazanovich,[1] and R.Sh. Tsvyk[1,3]**

[1]*Institute of Atmospheric Optics,*
*Siberian Branch of the Russian Academy of Sciences, Tomsk*
[2]*Institute of Theoretical and Applied Mechanics,*
*Siberian Branch of the Russian Academy of Sciences, Novosibirsk*
[3]*Tomsk State University*

The results of measurements of intensity fluctuations of a laser beam crossing the supersonic gas flow in aerodynamic tunnel T-326 at the Institute of Theoretical and Applied Mechanics SB RAS are described. It has been established that the intensity of gas flow density turbulent pulsations far exceeds the intensity of the atmospheric pulsations and increases with increasing gas compressibility. The spectral density of the sensing beam intensity has a high frequency maximum. The frequency range, where this maximum is located, determines the characteristic scales of density turbulent inhomogeneities arising in a compressible gas flow. The range of characteristic scales of turbulent density inhomogeneities in the flow is expanded with pressure increase.

## Introduction

Supersonic flows belong to a wide range of turbulent flows, which have a nonstationary organized motion of weakly pulsed large scale formations (great vortices) with a stable and spatial-temporal shape against the background of disordered small scale velocity fluctuations.[1–3] As can be seen from the schlieren photographs in Fig. 1, the supersonic gas flow is divided into zones, which contours are determined by gradients of mean density (index of refraction) of the medium. Several uniform structures are formed along the flow axis. The number of these structures is defined by the initial velocity of the flow escape. The turbulence intensity, minimal in the first structure, increases in every next one. In the transverse direction we also observe the mean density distribution inhomogeneity in the flow.

Mean characteristics of the flow were investigated rather well both theoretically and experimentally. Characteristic properties of the turbulence in supersonic flows were studied insufficiently. At the same time just the turbulent regime determines the structure of supersonic flow passing around the obstacles that should be taken into account when developing the high-speed aircrafts.

To investigate the turbulence in supersonic flows, the use of optical methods is very promising, because of their remoteness, low-inertia, and non-introducing distortions to the flow structure as contact sensors. However, strong inhomogeneity of density fluctuations in the flow complicates the problem of reconstruction of the turbulence parameters from the optical measurements because in the methods of transmission[4] the optical radiation fluctuations are determined by fluctuations of the refractive index along the whole sensing path.
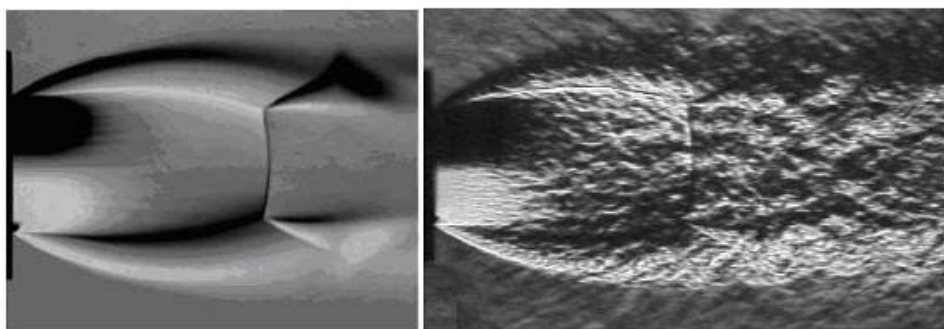


**Fig. 1.** Schlieren-photographs of the flow under study with a large (left) and small (right) exposure, *npr* = 9.

In the Refs. 5 and 6, the attempts to evaluate the variance of phase fluctuations of the optical wave propagated in a supersonic flow, based on the model of density fluctuations of a compressible gas developed in Ref. 7. Thus, a possibility of turbulence diagnostics is demonstrated in the supersonic flow by the transmission methods. However, in the optical wavelength range, where the radiation detectors, quadratic in field, are used, to measure phases, it is necessary to use complex reception circuits of the interferometric or heterodyne type to obtain the phase information based on the wave intensity measurements. It is more convenient for diagnostics of the results to use immediately the results of measuring the intensity of transmitting laser radiation. Just the intensity fluctuations of optical wave are most sensitive to small scale density fluctuations (or refractive index) of the medium. This paper presents the results of measurements of variance and intensity spectra of the laser beams propagating through a flow of compressible gas.

## Experimental stand. Equipment and measurement technique

The experiments were conducted using a jet module of the aerodynamic tunnel T-326 with a convergent nozzle. The Mach number $M$ at the nozzle cut was equal to 1, the diameter $d$ of the nozzle cut was 30 mm. The experiments were made at such pressures in the prechamber of the jet module that the following conditions were fulfilled: $npr = p_0/p_c = 5.0$ ($n = 2.64$) and $npr = 9$ ($n = 4.65$). Here $p_0$ is the pressure in the aerodynamic tube prechamber; $p_c$ is the pressure in the Eifelian chamber (operating section of the tube); $n$ is the degree of jet off-design (ratio between the static pressure in a jet at the nozzle cut and the pressure of the environment, that is, to the pressure in the Eifelian chamber). A simplified schematic representation of the aerodynamic tube and the block-diagram of the optical experiment are given in Fig. 2.

The measurements procedure was as follows. The laser radiation was emitted through the Eifelian chamber (with a cross section of 0.8×0.8 m) below the jet reflecting from a mirror of 300 mm in diameter and was directed to the photoreceiver so that a light beam passed through the jet. The laser beam initial diameter was 1 mm and the angular divergence was 1.5 milliradian. At the jet inlet the beam diameter was 7 mm. The radiation detector (photoelectric amplifier) and the source (He–Ne laser) were mounted at one optical table, where a vertical or horizontal position can be changed, that eliminated the necessity of the optical scheme tuning at every measurement. By table motion, the measurement point coordinates were determined: $x$ – along the axis relative to the nozzle cut (cross section) and $r$ – downwards vertically relative to the jet axis (radius). The coordinates of measurement points are given in Table 1. The jet radius at the nozzle cut was 15 mm.
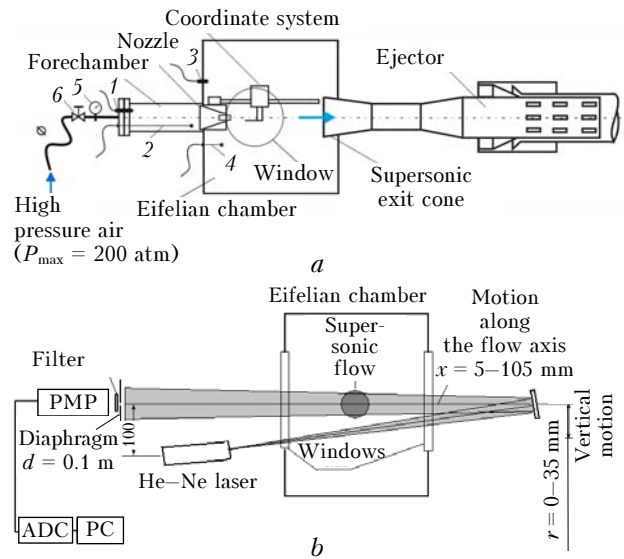


Fig. 2. Simplified scheme of the aerodynamic tunnel T-326 (*a*) and block-diagram of the experiment (*b*). *1* is the pressure detector in the forchamber; *2* is the temperature detector in the forchamber; *3* is the pressure detector in the Eifelian chamber; *4* is the temperature detector in the Eifelian chamber; *5* is the manometer; *6* is the pressure regulating valve in the forchamber (*a*).

**Table 1. Coordinates of measurement points**

| Cross section | $npr = 5$ | | | | $npr = 9$ | | | | |
|---|---|---|---|---|---|---|---|---|---|
| $x$, mm | 5 | 30 | 45 | 75 | 5 | 40 | 45 | 60 | 105 |
| Radius $r$, mm | 0 20 35 | 0 20 35 | 0 28 | 0 10 15 19 35 | 0 35 | 0 26 | 0 35 | 0 13 27 35 | 0 25 |

Realizations of laser radiation intensity with duration of 0.5 s at the numbering frequency 1 or 2 MHz were memorized in the computer. Simultaneously the jet parameters were recorded. At every point three realizations were recorded. Based on these realizations the variance and spectral density of intensity fluctuations were calculated.

## Results of measurements
### Conditions of propagation

The constructed flow diagram using the calculation density isolines, is shown in Fig. 3. Hanging jump *1*, interacting with the Mach disk *2*, forms the triple configuration of condensation jumps *1*, *2*, *3* and the mixing layer *4*. The jet boundary (mixing layer) is denoted by *5*.
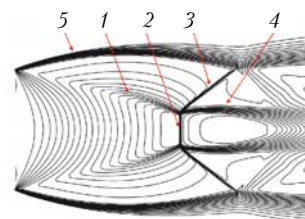


Fig. 3. The flow density structure in the jet, $npr = 5$.

Figure 4 shows the diagrams of the static pressure, density, and flow velocity in the cross section $x = 5$ mm along the radius $r = 0-30$ mm for the case $npr = 5$. Here $R$ is the radius of output cross section of the nozzle; $p$, $\rho$ are the static pressure and air density in the jet; $p_c$ and $\rho_c$ are the static pressure ($\sim 1$ atm) and air density in the surrounding medium (Eifelian chamber); $V$ is the velocity modulus, m/s.
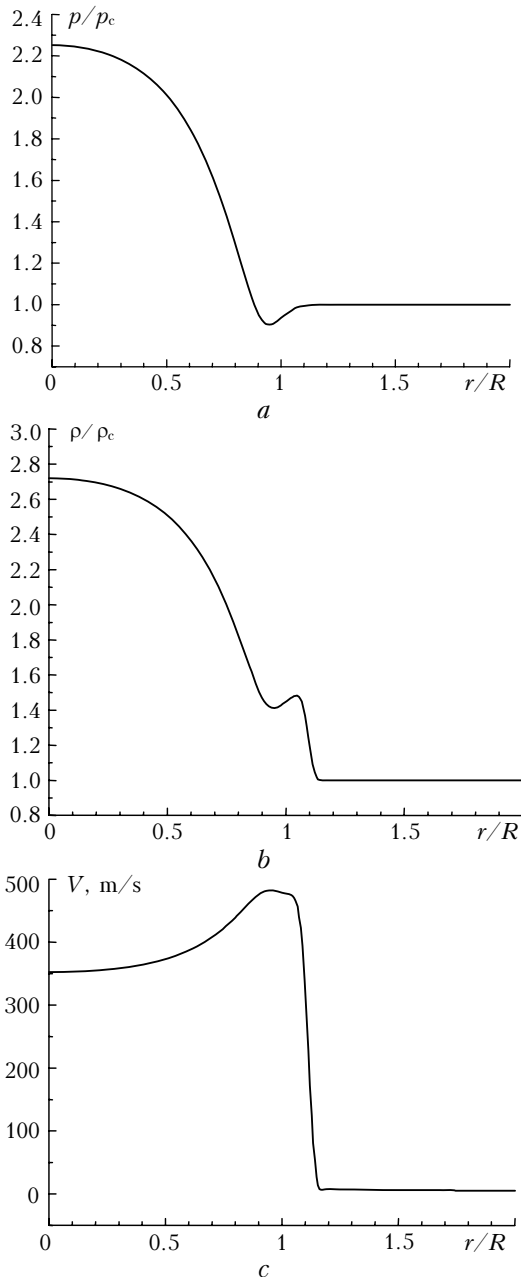


$a$



$b$



$c$

**Fig. 4.** Distribution of flow parameters in a cross section $x = 5$ mm along the radial coordinate for the case $npr = 5$; static pressure distribution (*a*); density distribution (*b*); flow velocity distribution (in absolute value) (*c*).

Thus, in the path of laser beam propagation one can differentiate three characteristic segments, which differ both in mean value and in the fluctuation level of the refractive index.

*The first*, the most extended segment is located in the Eifelian chamber outside the jet. At this segment the medium motion is practically lacking, the density and pressure are close to atmospheric ones; the density fluctuations are probably caused by sound waves generated by the jet. The length of this section by several tens of times exceeds the jet radius.

*The second*, small in length (several mm) and characterized by vast gradients of mean characteristics section of the path, is located in the external region of the jet mixing (region *5*, Fig. 3).

*The third* section of 30-40 mm length is located immediately in the jet and is characterized by the supersonic velocity of gas motion, high pressure, density and their gradients, including the pressure jumps — the Mach disks and internal regions of mixing (*4*, Fig. 3) and large, as compared with the other sections, turbulence intensity.

## Spectral density of intensity fluctuations

Figures 5 and 6 show examples of spectra of intensity fluctuations of a sounding laser beam. The values of spectral fluctuation density $U(f) = fW(f)$ are plotted on the $Y$-axis, where $W(f)$ is the beam intensity spectrum, calculated with the use of the fast Fourier transform (FFT). For comparison, straight lines are shown in the figures, which correspond to the slopes of laser radiation intensity spectra in the turbulent atmosphere in the region of low $U(f) \sim f$ and high $U(f) \sim f^{-5/3}$ frequencies for the Kolmogorov turbulence spectra.

From the spectra, shown in Figs. 5 and 6, it follows that the basic contribution in the laser radiation intensity fluctuations, propagated through the supersonic flow, is made by the inhomogeneities of the refractive index with two characteristic scales. The first scale is determined by the low frequency maximum of spectra at frequencies $f_{m1} \approx 900-1000$ Hz, when a laser beam propagates in the Eifelian chamber outside the jet, and $f_{m1} \approx 1000-1200$ Hz, when intersects it. The position of this maximum on the frequency axis depends weakly on the pressure and almost is not varied at variation of the parameter $npr$. The second scale at $npr = 5$ is determined by high-frequency spectral maximum at frequencies $f_{m2} \approx 30-60$ kHz. At $npr \approx 9$ the high-frequency maximum is less expressed than at $npr = 5$, i.e., with the pressure increase the size distribution of inhomogeneities of the refractive index, which make the basic contribution in high-frequency intensity fluctuations in a sounding beam, becomes more homogeneous. So, we can draw the conclusion that the size spectrum of density inhomogeneities in the compressed gas jet expands with pressure increase.

The slope of spectra in Figs. 5 and 6 in the frequency range $f < f_{m1}$ is determined roughly by the linear dependence of spectral density on the frequency $U(f) \sim f$. In the range $f > f_{m1}$ the spectrum decreases in accordance with the power function $U(f) \sim f^{-5/3}$ if the propagation occurs outside the

jet. The spectrum decrease in the high frequency range $f > f_{m2}$ at laser beam propagation through the jet is also close to the power function $f^{-5/3}$.

The power functions $U(f) \sim f$ and $U(f) \sim f^{-5/3}$ are characteristic for laser beam intensity fluctuation spectra in the turbulent atmosphere, when the regime of weak optical turbulence is realized on the path. This makes it possible to assess the typical scale of inhomogeneities of the refractive index, making basic contribution in the spectral density $U(f)$ in the region of low frequency maximum, as well as to use the relationship of the smooth perturbation method (SPM) [Ref. 8] valid for the regime of weak fluctuations in the atmosphere $f_{m1} \approx 0.4V/l_1$, where $V$ is the wind velocity transverse to the path; $l_1$ is the characteristic size of inhomogeneities. Having used $f_{m1} \approx 1$ kHz and the jet velocity $V \approx 330$ m/s, we find that $l_1 \approx 13.2$ cm. For the wind aerodynamic tunnel T-326 the sound frequency equals to 2.4 kHz [Ref. 2] that corresponds to a wavelength of 13.8 cm. The proximity of the assessment of $l_1$ to the sound wavelength generated by the jet T-326, enables one to

draw a rough conclusion that the inhomogeneities of the refractive index, which bring the basic contribution in the laser radiation fluctuations in the region of low-frequency maximum of spectral density, are initiated by sound waves.

At laser radiation propagation beyond the jet the spectral density value in the high-frequency maximum is much less than in the low-frequency one. When propagating through the jet the values of $U(f)$ in both maxima are equalized. The lesser values of spectrum in the high-frequency maximum range are conditioned by the fact that the path section, intersecting the jet, is less than the path length outside the jet by a factor of 60. The presence of weak high-frequency maximum at sounding beam propagation beyond the jet can be due to the interference of sound waves leading to the formation of small scaled inhomogeneities of the refractive index, which are observed at the Schlieren-photographs (Fig. 1). The spectral maximum in the frequency range higher than 300 kHz takes place because of inadequate resolution of signal numbering in this frequency range.
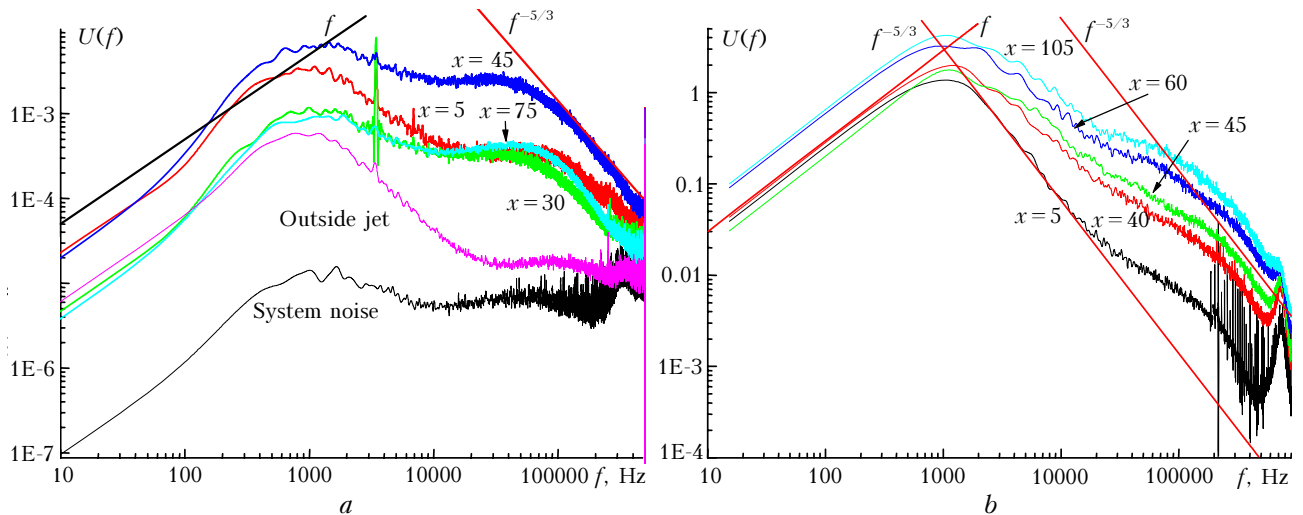


**Fig. 5.** Spectral density of intensity fluctuations in different flow cross sections at $r = 0$: $npr = 5$ ($a$); $npr = 9$ ($b$).
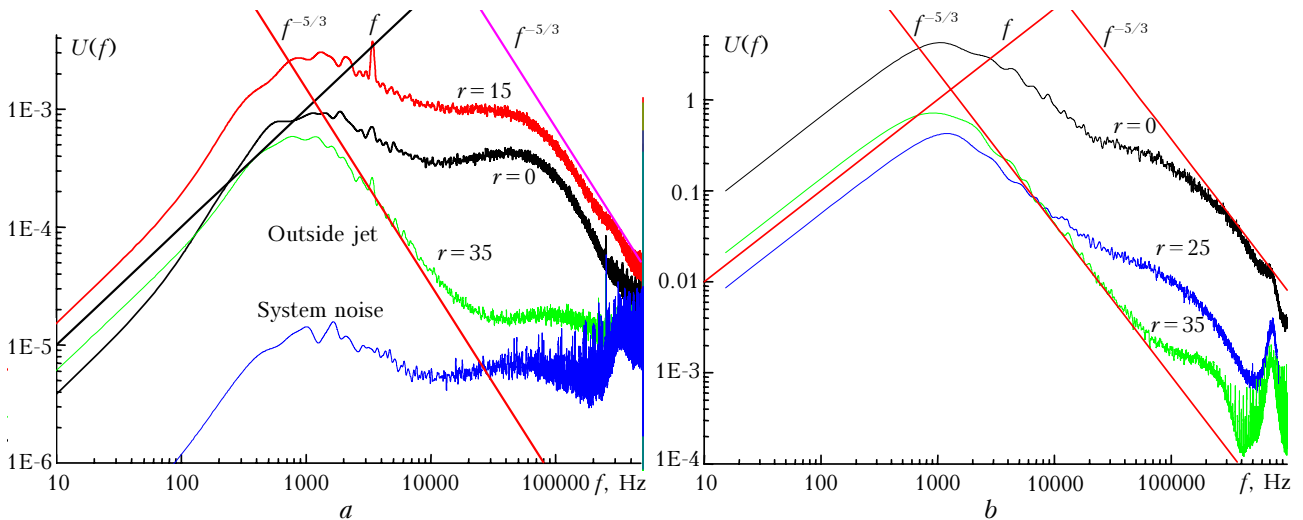


**Fig. 6.** Spectral density of intensity fluctuations at the measurement point displacements in a chosen cross section relative to the flow axis: $npr = 5$, $x = 75$ mm ($a$); $npr = 9$, $x = 105$ mm ($b$).

## Variance of intensity fluctuations

Figure 7 shows measurements of relative variance

$$\sigma^2 = \left( <I^2> / <I>^2 \right) - 1,$$

of intensity fluctuations of laser radiation passed through the supersonic jet, where $I$ is the intensity on the beam axis; the averaging over the ensemble is denoted by French quotes.

The measurements were made for two distribution geometries: 1) laser beam intersects the jet centre; 2) laser beam passes at a distance of 35 mm from the jet axis and in the absence of the jet along the same paths with closed doors of the Eifelian chamber. In the latter case the variance was practically equal to zero, $\sigma^2 \approx 0.00006$.

Consider that the turbulent motion in the jet can be described on the basis of the theory of developed turbulence in the atmosphere,[8] as well as assume the use of the formula $\sigma^2 = 1.23 C_n^2 k^{7/6} L^{11/6}$ of the first approximation of SPM for calculating the variance of intensity fluctuations in the jet, where $k = 10^5$ cm$^{-1}$; $L = 170$ cm is the path length in the Eifelian chamber and $L = 3$ cm in the jet. Then we can assess the integral over the path structural characteristic of fluctuations of the refractive index $C_n^2$ from the results of variance measurements.

Table 2 shows the results of measurement of intensity variance and the evaluation of integral values of $C_n^2$ in the Eifelian chamber for the paths $r = 0$ and $r = 35$, as well as the values of $\Delta\sigma^2$ calculated as the difference of variances at these paths. On the assumption that the difference variance is associated with the effect of fluctuations in the jet, the values of $\Delta C_n^2$ in the jet, which are given in the line $\Delta\sigma^2$ of the table, are calculated for a path length in a jet of 3 cm.

From the results shown in Fig. 7 and Table 2 it follows that the increase of pressure (parameter $npr$) in the jet results in the essential increase of laser beam intensity fluctuations. The level of fluctuations depends highly on the jet region, through which the sounding beam passes. On the axis close to the nozzle cut, the jet fluctuations are minimal, increasing when receding from it. Some increase of fluctuations is observed close to the Mach disk, which is probably connected with random changes of the position of compression jump. At removal of the sounding path from the jet, the fluctuations decrease. Integral values of structural characteristic of fluctuations of the refractive index in the Eifelian chamber reach $C_n^2 \approx 10^{-11} - 10^{-12}$ cm$^{-2/3}$ that is by one or two orders of magnitude higher than the maximal values in the atmosphere. In the jet itself the values of the structural characteristic are higher: $C_n^2 \approx 10^{-9} - 10^{-10}$ cm$^{-2/3}$.

## Conclusion

From a comparison of obtained data with the similar measurements in the atmosphere it follows that the turbulent pulsations of gas density in the flow far exceed in value the atmospheric fluctuations and intensify with the increase of gas compressibility. The spectral density of beam intensity has a high-frequency maximum, which position on the frequency axis enables us to judge the size spectra of density inhomogeneities occurring in the compressed gas flow. With the pressure increase the spectrum of density inhomogeneities in the gas flow becomes more uniform. The determination of size distribution of gas density inhomogeneities in the flow requires more precision measurements and further development of optical fluctuation models in the compressed gas flow. These investigations are planned to start in the future.

### Acknowledgements

**Table 2. The measurements of $\sigma^2$ and $C_n^2$ along the axis and outside the flow**

| Parameter | Cross section $x$, mm | | | | | | | |
|---|---|---|---|---|---|---|---|---|
| | 5 | | 30 | | 45 | | 105 | |
| | Radius $r$, mm | | | | | | | |
| | 0 | 35 | 0 | 35 | 0 | 35 | 0 | 35 |
| *npr* = 5 | | | | | | | | |
| $\sigma^2$ | 0.0026 | 0.0018 | 0.0083 | 0.0071 | – | – | 0.007 | 0.002 |
| $C_n^2$, cm$^{-2/3}$ | $2.5\cdot10^{-13}$ | $1.7\cdot10^{-13}$ | $8.1\cdot10^{-13}$ | $6.9\cdot10^{-13}$ | – | – | $6.9\cdot10^{-13}$ | $1.7\cdot10^{-13}$ |
| $\Delta\sigma^2$ | 0.0008 | – | 0.0012 | – | – | – | 0.005 | – |
| $\Delta C_n^2$, cm$^{-2/3}$ | $1.2\cdot10^{-10}$ | – | $1.9\cdot10^{-10}$ | – | – | – | $8.0\cdot10^{-10}$ | – |
| *npr* = 9 | | | | | | | | |
| $\sigma^2$ | 0.022 | 0.013 | – | – | 0.038 | 0.02 | 0.047 | 0.021 |
| $C_n^2$, cm$^{-2/3}$ | $2.2\cdot10^{-12}$ | $1.2\cdot10^{-12}$ | – | – | $3.8\cdot10^{-12}$ | $1.9\cdot10^{-12}$ | $4.6\cdot10^{-12}$ | $2.1\cdot10^{-12}$ |
| $\Delta\sigma^2$ | 0.009 | – | – | – | 0.018 | – | 0.026 | – |
| $\Delta C_n^2$, cm$^{-2/3}$ | $1.4\cdot10^{-9}$ | – | – | – | $2.9\cdot10^{-9}$ | – | $4.1\cdot10^{-9}$ | – |

V.A. Banakh et al.

Vol. 20, No. 5 /May 2007/ Atmos. Oceanic Opt. 373

# References

1. O.M. Belotserkovskii, A.M. Oparin, and V.M. Chechetkin, *Turbulence: New Approaches* (Nauka, Moscow, 2002), 288 pp.
2. S.A. Gaponov and A.A. Maslov, eds., *Jet and Nonstationary Flows in Gas Dynamics* (SB RAS Press, Novosibirsk, 2000), 200 pp.
3. G.S. Samoilovich, *Hydro-Gas Dynamics* (Mashinostroenie, Moscow, 1990), 384 pp.
4. V.E. Zuev, V.A. Banakh, and V.V. Pokasov, *Optics of the Turbulent Atmosphere* (Gidrometeoizdat, Leningrad, 1988), 272 pp.
5. O. Pade, in: *Proc. of the 41st Israeli Conference on Aerospace Sciences* (Hifa, 2001).
6. O. Pade, Proc. SPIE **5981** (2005).
7. A. Yoshizewa, Phys. Fluids **7**, No. 12, 3105–3117 (1995).
8. V.I. Tatarskii, *Wave Propagation in the Turbulent Atmosphere* (Nauka, Moscow, 1967), 580 pp.